arXiv:1606.05782v1 [cond-mat.mtrl-sci] 18 Jun 2016

Magnetization reversal in mixed ferrite-chromite perovskites with non magnetic cation on the A-site

Orlando V. Billoni,[1,*] Fernando Pomiro,[2,†] Sergio A. Cannas,[1,‡]
Christine Martin,[3,§] Antoine Maignan,[3,¶] and Raul E. Carbonio[2,**]

[1] *Facultad de Matemática, Astronomía, Física y Computación, Universidad Nacional de Córdoba and Instituto de Física Enrique Gaviola (IFEG-CONICET), Ciudad Universitaria, 5000 Córdoba, Argentina.*
[2] *INFIQC (CONICET – Universidad Nacional de Córdoba), Departamento de Fisicoquímica, Facultad de Ciencias Químicas, Universidad Nacional de Córdoba, Haya de la Torre esq. Medina Allende, Ciudad Universitaria, X5000HUA Córdoba, Argentina.*
[3] *Laboratoire CRISMAT, UMR 6508 CNRS/ENSICAEN/UCBN, 6 Boulevard Marechal Juin, 14050 Caen cedex, France.*

(Dated: June 21, 2016)

In this work, we have performed Monte Carlo simulations in a classical model for $RFe_{1-x}Cr_xO_3$ with R=Y and Lu, comparing the numerical simulations with experiments and mean field calculations. In the analyzed compounds, the antisymmetric exchange or Dzyaloshinskii-Moriya (DM) interaction induced a weak ferromagnetism due to a canting of the antiferromagnetically ordered spins. This model is able to reproduce the magnetization reversal (MR) observed experimentally in a field cooling process for intermediate x values and the dependence with x of the critical temperatures. We also analyzed the conditions for the existence of MR in terms of the strength of DM interactions between Fe^{3+} and Cr^{3+} ions with the x values variations.

PACS numbers: 75.10.Hk,75.40.Mg,75.50.Ee,75.60.Jk
Keywords: Classical spin models, Perovskites, Magnetization reversal, DM interactions

INTRODUCTION

Some magnetic systems when cooled in the presence of low magnetic fields show magnetization reversal (MR). At high temperatures the magnetization points in the direction of the applied field while at a certain temperature the magnetization reverses, becoming opposite to the magnetic field in a low temperature range. In particular, this phenomenon has been observed in orthorhombic (space group: *Pbnm*) perosvkites like RMO_3 with R=rare earth or yttrium and M=iron, chromium or vanadium[1–8]. These materials exhibit a weak ferromagnetic behavior below the Néel temperature (T_N), arising from a slight canting of the antiferromagnetic backbone. The weak ferromagnetism (WFM) observed in these compounds can be due to two mechanisms related with two different magnetic interactions: antisymmetric exchange or Dzyaloshinskii-Moriya interaction (DM) and single-ion magnetocrystalline anisotropy[9,10]. In particular, in orthochromites $RCrO_3$ and orthoferrites $RFeO_3$ the WFM is due mainly to DM interactions[9].

MR was also observed in several ferrimagnetic systems such as spinels[11,12], garnets[13], among others. In these materials, MR has been explained by a different temperature dependence of the sublattice magnetization arising from different crystallographic sites, as predicted by Néel for spinel systems. However, this explanation cannot be applied to the orthorhombic perovskites with formula $RM_{1-x}M'_xO_3$ where R is a nonmagnetic ion (for example Y^{3+} or Lu^{3+}), because the magnetic ions occupy a single crystallographic site. In the case of YVO_3, the origin of MR has been explained based on a competition between DM interaction and single-ion magnetic anisotropy[14].

Some years ago, the presence of MR was also reported in polycrystalline perovskites with two magnetic transition ions randomly positioned at the B-site and non magnetic R cation at the A site. Some examples are $BiFe_{0.5}Mn_{0.5}O_3$, $LaFe_{0.5}Cr_{0.5}O_3$, $YFe_{0.5}Cr_{0.5}O_3$ and $LuFe_{0.5}Cr_{0.5}O_3$[15–18]. In a work by Kadomtseva et al. [1] the DM interactions were successfully used to explain the anomalous magnetic properties of single-crystal $YFe_{1-x}Cr_xO_3$ with different Cr contents. They showed that these compounds are weak ferrimagnets with a mixed character of the DM interaction. Moreover, the competing character of DM interactions is used in a mean field (MF) approximation by Dasari et al. [6] to explain the field cooling curves of polycrystalline $YFe_{1-x}Cr_xO_3$ for $0 \leq x \leq 1$. In their work the dependence of magnetization as a function of temperature, for the entire range of composition, is explained from the interplay of DM interactions of the Fe–O–Fe, Cr–O–Cr and Cr–O–Fe bounds. At intermediate compositions (x=0.4 and 0.5) MR is also reported in this work.

Numerical simulations have been proved to be useful to model magnetic properties of perovskites. Several studies of magnetic perovskites have been performed using Monte Carlo simulations (MC)[19–21], for instance, to characterize the critical behavior in yttrium orthoferrites[19] and in $La_{2/3}Ca_{1/3}MnO_3$[20,21]. However, to the best or our knowledge, MR has not been studied using MC simulations. In the case of solid solutions, MC simulations can take into account fluctuations in the distribution of atomic species and thermal fluctuation that cannot be considered in mean field models.

In this work we have performed MC simulations using a classical model for $RFe_{1-x}Cr_xO_3$ with R = Y or Lu, comparing the numerical simulations with experiments and mean field calculations[6,22]. We also adapted MF approximations to test our MC simulations. This model is able to reproduce the magnetization reversal (MR) observed in a field cooling process for intermediate x values and the dependence on x of the critical temperature.

We also analyzed the conditions for the existence of MR in terms of the strength of DM interactions between Fe^{3+} and Cr^{3+} and the chromium content.

I. METHODS

Neutron diffraction studies have shown that the magnetic structure of $RFe_{1-x}Cr_x0_3$ compounds with a nonmagnetic R ion (space group :$Pbnm$) is $\Gamma_4(G_x, A_y, F_z)$ in the Bertaut notation[23]. In this structure the moments are oriented mainly in an AFM type-G arrangement along the x-direction. A nonzero ferromagnetic component along the z-axis (canted configuration) and an AFM type-A arrangement along the y-axis are allowed by symmetry[9,24].

We model the $RFe_{1-x}Cr_xO_3$ perosvkites, with R=Lu or Y using the following Hamiltonian of classical Heisenberg spins lying in the nodes of a cubic lattice with $N = (L \times L \times L)$ sites,

$$\mathcal{H} = -\frac{1}{2}\sum_{\langle i,j\rangle}[J_{ij}\vec{S}_i \cdot \vec{S}_j + \vec{D}_{ij} \cdot (\vec{S}_i \times \vec{S}_j)] - \sum_i K_i (S_i^x)^2 - H\sum_i m_i S_i^z, \quad (1)$$

where $\langle ...\rangle$ means a sum over the nearest neighbor sites and $\vec{S}_i$ are unitary vectors. $J_{ij} < 0$ takes into account the superexchange interaction and $\vec{D}_{ij}$ the antisymmetric Dzyalshinskii-Moriya interactions, where this vector points in the $\hat{j}$ direction. Due to the collective tilting of the (Fe,Cr)O_6 octahedra the DM interaction is staggered. H correspond to the external applied field and is expressed as, $H = B\mu_{Fe}/k_B$, where B is the external field and $\mu_{Fe} = g\mu_B S_{Fe}$ with $g = 2$ the gyromagnetic factor constant, μ_B the Bohr magneton and $S_{Fe} = 5/2$ is the total spin of Fe3+ ion –equivalently $S_{Cr} = 3/2$ for Cr3+ ion. Then, $m_i = 1$ for then Fe^{3+} ions and $m_i = S_{Cr}/S_{Fe} = 0.6$ for the Cr^{3+} ions. Both interactions, J_{ij} and D_{ij}, depend on the type of ions (Fe^{3+} or Cr^{3+}) that occupy sites i and j, so each pair interaction can take three different values. Suppose that site 1 is occupied by Cr^{3+} and site 2 by Fe^{3+} ion, then the super-exchange interaction couplings are $J_{22} = 2S_{Fe}^2 J_{FeFe}/k_B$, $J_{12} = J_{21} = 2S_{Fe}S_{Cr}J_{FeCr}/k_B$ and $J_{11} = 2S_{Cr}^2 J_{CrCr}/k_B$, where $J_{\alpha\beta}$ – with $\alpha, \beta =$ Cr or Fe – are the exchange integrals. In the case of DM interactions $D_{22} = S_{Fe}^2 D_{FeFe}/k_B$; $-D_{12} = D_{21} = S_{Fe}S_{Cr}D_{FeCr}/k_B$ and $D_{11} = S_{Cr}^2 D_{CrCr}/k_B$. Finally, the single site interactions corresponding to the uniaxial anisotropy are $K_1 = S_{Cr}K_{Cr}/k_B = K_2 = S_{Fe}K_{Fe}/k_B > 0$ which point in the x direction. k_B is the Boltzmann constant. For simplicity we consider the same anisotropy for Cr^{3+} and Fe^{3+} ions.

A. Monte Carlo methods

We performed Monte Carlo simulations using a Metropolis algorithm. Along this work we considered a cubic lattice with $N = 40 \times 40 \times 40$ sites and open boundary conditions. In order to simulate $RFe_{1-x}Cr_xO_3$ compounds the sites of the cubic lattice are occupied by Cr^{3+} ions with probability x, and with probability $(1-x)$ by the Fe^{+3} ions. Since all the super-exchange interactions are antiferromagnetic the system can be divided into two sublattices A and B, each one ferromagnetically ordered in the $\hat{i}$ direction and opposite to the other. We computed the sublattice magnetization,

$$\vec{m}_\alpha = \frac{1}{N}\sum_{\vec{S}_i \in \{\vec{S}_\alpha\}} \vec{S}_i, \quad (2)$$

where $\{\vec{S}_\alpha\}$ with $\alpha = A, B$ is the set of spins belonging to sublattice A or sublattice B, and the susceptibility,

$$\chi_\alpha = (\frac{N}{k_B T})(\langle m_\alpha^2\rangle - \langle m_\alpha\rangle^2), \quad (3)$$

where $\langle ...\rangle$ means a thermal average. At each temperature we equilibrated the system using 10^5 Monte Carlo steps (MCS). After that we get the thermal averages using another 10^5 MCS, measuring the quantities (e.g. the magnetization) every 10^2 MCS. From the peak of the susceptibility we obtained the critical temperature as function of the Chromium content for $x = 0, 0.1, 0.2, ..., 1$. As we will explain later, the values of the J_{11} and J_{22} interactions were chosen in order to reproduce the Néel temperature T_N of the pure compounds, $RCrO_3$ and $RFeO_3$, respectively. J_{12} were considered as a free parameter, to be fitted from the experiments. The value used for $K_1 = K_2$ in all the simulations was $K_1 = 7 \times 10^{-3} J_{22}$[19]. In the case of $LuFe_{1-x}Cr_xO_3$ we used the following values for the DM interactions $D_{11} = 0.74 \times 10^{-2} J_{22}$ and $D_{22} = 2.14 \times 10^{-2} J_{22}$, taken from Refs.[25] and [26], respectively. There is no estimation of D_{12} in the literature, so we assume as a reference the value $D_{12} = -1.7 \times 10^{-2} J_{22}$ to obtain the critical temperatures, considering that a similar value was obtained by Dasari et al[6] fitting $YFe_{1-x}Cr_xO_3$ data. Since DM interactions are considerably lower than super-exchange interactions, small variations of this interactions does not substantially affect the antiferromagnetic ordering temperatures.

B. Effective model

In order to get a deeper physical insight about the low temperature behavior of these systems, we compared the MC results against an effective model that generalizes some ideas introduced by Dasari et al[6]. In this model a site i is occupied with probability $P_1[x] = P_{Cr}[x] = x$ by a Cr^{3+} ion and with probability $P_2[x] = P_{Fe}[x] = (1-x)$ by a Fe^{3+} ion. The energy, in a two-sublattice approximation, is then given by

$$\begin{aligned} E = z[&\mathcal{J}_{11}\vec{M}_1^A\cdot\vec{M}_1^B + \mathcal{J}_{22}\vec{M}_2^A\cdot\vec{M}_2^B + \\ &+ \mathcal{J}_{12}(\vec{M}_1^A\cdot\vec{M}_2^B + \vec{M}_2^A\cdot\vec{M}_1^B) + \\ &+ \mathcal{D}_{11}\cdot(\vec{M}_1^A\times\vec{M}_1^B) + \mathcal{D}_{22}\cdot(\vec{M}_2^A\times\vec{M}_2^B) + \\ &+ \mathcal{D}_{12}\cdot(\vec{M}_1^A\times\vec{M}_2^B + \vec{M}_2^A\times\vec{M}_1^B)] + \\ &- \mathcal{K}_1[(M_{1x}^A)^2 + (M_{1x}^B)^2] - \mathcal{K}_2[(M_{2x}^A)^2 + (M_{2x}^B)^2)] + \\ &- \mathcal{H}_1[M_{1z}^A + M_{1z}^B] - \mathcal{H}_2[M_{2z}^A + M_{2z}^B], \end{aligned} \quad (4)$$

here $\vec{M}_1^\alpha$, with $\alpha = A$ or B is the total magnetization of the chromium ions belonging to the sublattice, A or B, respectively, and $\vec{M}_2^\alpha$ is the total magnetization of the iron ions belonging to the sublattice, A or B, respectively. $\mathcal{J}_{ij} = P_i[x]P_j[x]J_{ij}$, $\mathcal{D}_{ij} = P_i[x]P_j[x]D_{ij}$, $\mathcal{K}_i = P_i[x]K_i$, and $\mathcal{H}_i = m_iP_i[x]H$ with $m_1 = 0.6$ and $m_2 = 1$. Let ϕ and θ the canting angles of M_1 and M_2 respectively (see figure 1). z is the number of nearest neighbors.

For small canting angles, disregarding constant terms, the energy is

$$\begin{aligned} E = &2\mathcal{J}_{11}\phi^2 + 2\mathcal{J}_{22}\theta^2 + \mathcal{J}_{12}(\theta+\phi)^2 - 2\mathcal{D}_{11}\phi - 2\mathcal{D}_{22}\theta + \\ &+ 2\mathcal{D}_{12}(\theta+\phi) + 2\mathcal{K}_1\phi^2 + 2\mathcal{K}_2\theta^2 - 2\mathcal{H}_1\phi - 2\mathcal{H}_2\theta. \end{aligned} \quad (5)$$

The minimum energy configuration is obtained from

$$\begin{aligned} \frac{\partial E}{\partial\theta} &= 4\mathcal{J}_{22}\theta + 2\mathcal{J}_{12}(\theta+\phi) - 2\mathcal{D}_{22} + \mathcal{D}_{12} + 4\mathcal{K}_2\theta + \\ &- 2\mathcal{H}_2 = 0 \\ \frac{\partial E}{\partial\phi} &= 4\mathcal{J}_{11}\phi + 2\mathcal{J}_{12}(\theta+\phi) - 2\mathcal{D}_{11} + \mathcal{D}_{12} + 4\mathcal{K}_1\phi + \\ &- 2\mathcal{H}_1 = 0. \end{aligned}$$

Solving these two equations for θ and ϕ we can obtain the magnetization per site as function of x as:

$$M_z(x) = \mu_{cr}P_1[x]\phi(x) + \mu_{Fe}P_2[x]\theta(x). \quad (6)$$

In order to compare with MC simulations we define the reduced magnetization $m_z = M_z/\mu_{Fe}$. For $x = 0$, $P_2 = 1$ and $P_1 = 0$ we have

$$m_z = \frac{D_{22} + m_2H}{2(J_{22} + K_2)}m_2, \quad (7)$$

and for $x = 1$, $P_2 = 0$ and $P_1 = 1$, so

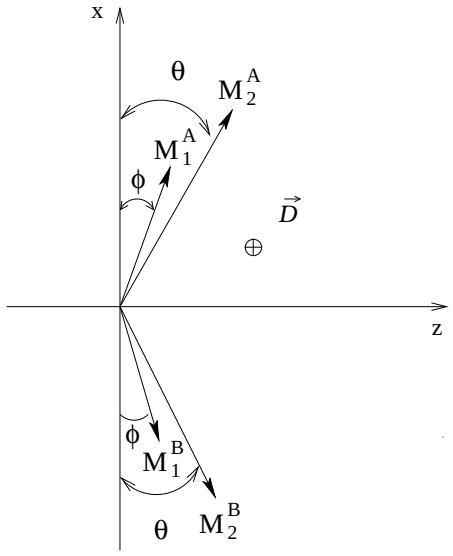

FIG. 1. Sketch of the configuration of the two sublattice magnetization.

$$m_z = \frac{D_{11} + m_1H}{2(J_{11} + K_1)}m_1. \quad (8)$$

These are the zero temperature –weak– magnetization for the pure compounds, $LuFeO_3$ and $LuCrO_3$, respectively.

C. Experiments

$LuFe_{1-x}Cr_xO_3$ ($x = 0.15, 0.5$ and 0.85) samples were prepared in polycrystalline form by a wet chemical method. A very reactive precursor was prepared starting from an aqueous solution of the metal ions and citric acid. Stoichiometric amounts of analytical grade Lu_2O_3, $Fe(NO_3)_3\cdot 9H_2O$ and $Cr(NO_3)_3\cdot 9H_2O$ were dissolved in citric acid and some drops of concentrated HNO_3, to facilitate the dissolution of Lu_2O_3. The citrate solution was slowly evaporated, leading to an organic resin that contained a homogeneous distribution of the involved cations. This resin was dried at 120 ^{o}C and then decomposed at 600 ^{o}C for 12 h in air, with the aim of eliminate the organic matter. This treatment produced homogeneous and very reactive precursor materials that were finally treated at 1050 ^{o}C in air for 12 h. $LuFe_{1-x}Cr_xO_3$ compounds were obtained as orange, well-crystallized powders as shown in Ref.[18]. The magnetic measurements were performed using a commercial MPMS-5S superconducting quantum interference device magnetometer, on powdered samples, from 5 to 400K, and for the 300 to 800K measurements the VSM option was used in the same MPMS.

II. RESULTS

A. Antiferromagnetic ordering temperature

The analysis of the solid solution Néel temperature $T_N(x)$ of $LuFe_{1-x}Cr_xO_3$ as a function of the Cr concentration allowed us to estimate the coupling constants of the model as follows.

The critical temperature obtained from MC in our model for $x = 0$ ($LuFeO_3$) is $\frac{T_N}{J_{22}} = 1.44$. Considering that the measured Néel temperature[27] is $T_N = 628$ K, then the value for the superexchange interaction between the Fe^{+3} ions that reproduces the experimental result in our model is: $J_{22} = 436$ K. Similarly, for $x = 1$ ($LuCrO_3$), $T_N = 115$ K[28] and then $J_{11} = 79.8$ K. In our analysis the value of J_{12} is a fitting parameter and it will be extracted from the approach of MC simulations and the experimental results. Namely, we choose the value of J_{12} which provides an MC curve $T_N(x)$ that minimized the sum of the mean square deviations respect to the available experimental results.

Previous estimations of the solid solution Néel temperature $T_N(x)$ in this kind of compounds were based on mean field approximations, in which DM interactions were neglected[6,22]. For instance, Dasari et al.[6] obtained

$$T_N = \frac{z}{3}\left(\sum_{i=1,j=1}^{2} J_{ij}^2 P_i[x]^2 P_j[x]^2\right)^{\frac{1}{2}}, \qquad (9)$$

where z is the number of nearest neighbors, J_{ij} and $P_i[x]$, with $i, j = 1, 2$ where already defined in Sections I A and I B. In a cubic lattice $z = 6$, so for the pure compounds ($x = 0$ or $x = 1$) $T_{N_i} = \frac{z}{3} J_{ii}$ and therefore

$$T_N = \sqrt{T_{N_1}^2 P_1[x]^4 + 8J_{12}^2 P_1[x]^2 P_2[x]^2 + T_{N_2}^2 P_2[x]^4}. \qquad (10)$$

In a different mean field approximation Hashimoto[22] obtained the expression

$$T_N = \frac{1}{2}\left[P_1[x]T_{N_1} - P_2[x]T_{N_2} + \sqrt{(P_1[x]T_{N_1} + P_2[x]T_{N_2})^2 + 4P_1[x]P_2[x](\frac{4z^2}{9}J_{12}^2 - T_{N_1}T_{N_2})}\right]. \qquad (11)$$

The dependence of the Néel temperature on the Cr content obtained from experiments in polycrystals is shown in Fig. 2. The values $x = 0$[27], $x = 1$[28] were taken from the literature, and $x = 0.15, 0.5$ and 0.85 were sinthetized in our experiments. In this figure we also compare the best fittings of the experimental results obtained from the MC simulations and using Eqs. (10) and (11).

From Hashimoto and Dasari expressions very different values of J_{12} are obtained, 11 K and 162 K respectively. The value derived from the MC simulations is $J_{12} = 106$ K, which is in between the values obtained from Eqs.(11) and(10). Considering that the value of the exchange integral $J_{FeCr} = J_{12}/(2S_{Cr}S_{Fe})$ where $S_{Cr}^2 = S_{Cr}(S_{Cr}+1)$ and $S_{Fe}^2 = S_{Fe}(S_{Fe}+1)$ we obtain $J_{FeCr} = 28,3$ K, $J_{FeCr} = 1.9$ K and $J_{FeCr} = 9.25$ K from Eq. (11), Eq. (10) and MC simulations, respectively. The value of J_{FeCr} reported by Dasari et al [6] for $YFe_{1-x}Cr_xO_3$ ($J_{FeCr} = 24.3$ K) is comparably to the value we have found for $LuFe_{1-x}Cr_xO_3$ using the same equation. The value reported by Kadomtseva et al. for $YFe_{1-x}Cr_xO_3$ monocrystals using Eq. (11) ($J_{FeCr} = 6,64$ K) is considerably lower than the value reported by Dasari et al. in the same compound.

In order to test the mean field approximations, we fitted the MC results with the corresponding expressions (10) and (11). In figure 3 we show a fit of the Néel temperatures obtained from MC simulation using Eq.(10). From this fit we obtained $J_{12} = 306$ K which is considerably greater than the value used in MC simulations $J_{12} = 106$ K. For comparison we included in Fig. 3 a plot of the mean field expression using the MC simulation value ($J_{12} = 106$ K). One can observe that with this value Eq.(10) clearly departs from the results of MC simulations. We concluded that a fit with expression (10) always overestimates the value of the exchange interaction J_{12}. Similarly, fitting the MC results using Eq.(11) systematically underestimates J_{12}. The accuracy of MF model is expected to be good in low and high Cr content; at intermediate concentrations the effect of the distribution of the interactions is important. Then, a fit which takes into account all the concentration range somehow biases the value of the J_{12} interaction.

In figure 4 we show experimental data for the critical temperature of $YFe_{1-x}Cr_xO_3$ as a function of the chromium content reported by Dasari et al.[6]. We also show the data obtained from MC simulations with $J_{FeCr} = 9.25$ K tuned to get the best fit with the experimental points. We also include a plot of the mean field expression derived by Dasari et al.[6] using the value $J_{FeCr} = 24.0$ K which is the value reported by these authors. Finally, a plot of Hashimoto's expression[22] Eq.(11) using the value of $J_{FeCr} = 6.64$ K reported by Kadomtseva et al[1] is also included. In this last work the samples studied were single monocrystals of the $YFe_{1-x}Cr_xO_3$ compound. MC approach gives a very good agreement with the experiments in all the range of concentrations and the value obtained for $J_{FeCr} = 9.25$ K is higher

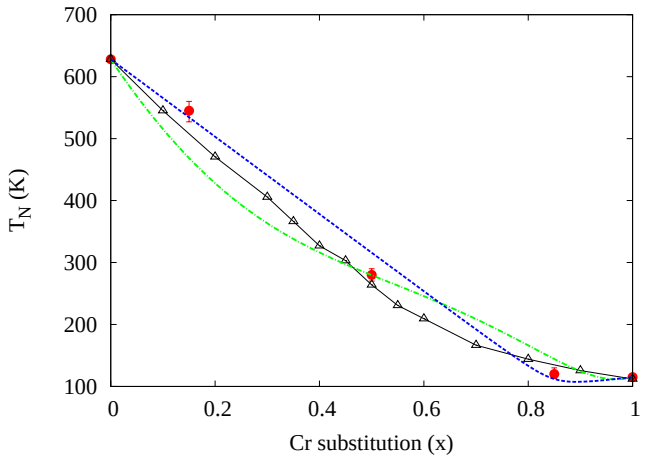

FIG. 2. (Color online) Néel temperature as function of the fraction of Cr. Full red circles correspond to the experiments with $LuFe_{1-x}Cr_xO_3$, and open triangles to MC simulations. The lines correspond to fits of the experiments using Eq.(10) (blue dashed lines) and Eq.(11) (green dot dashed lines), giving $J_{12} = 162$ K and $J_{12} = 11$ K, respectively. The parameter values of the MC simulation were $J_{22} = 436$ K, $J_{11} = 79.8$ K, and $J_{12} = 106$ K.

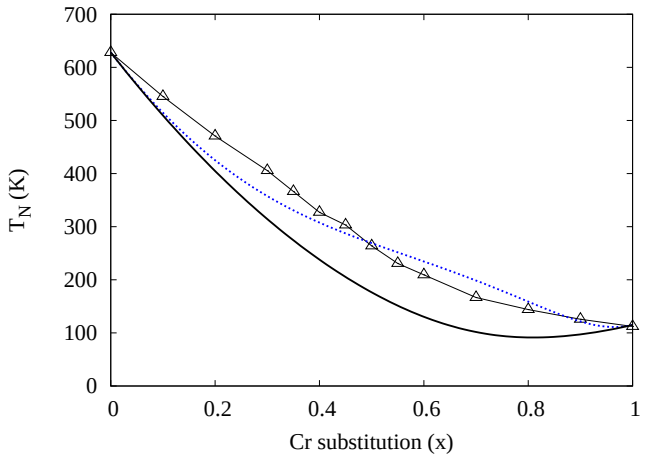

FIG. 3. (Color online) Néel temperature as function of the fraction of Cr for $LuFe_{1-x}Cr_xO_3$. Open triangles correspond to MC simulations and the blue dotted line corresponds to a fit of the MF expression Eq. (10). The parameter that results from the fit is $J_{12} = 306$ K. The full line corresponds to a plot of Eq. (10) using the value of MC simulations ($J_{12} = 106$).

than the reported by Kadomtseva et al. and lower than the reported by Dasari et al. Finally, the values J_{FeCr} obtained from MC for both compounds $YFe_{1-x}Cr_xO_3$ and $LuFe_{1-x}Cr_xO_3$ are the same, indicating that the exchange integral is not substantially affected by the substitution of yttrium by lutetium.

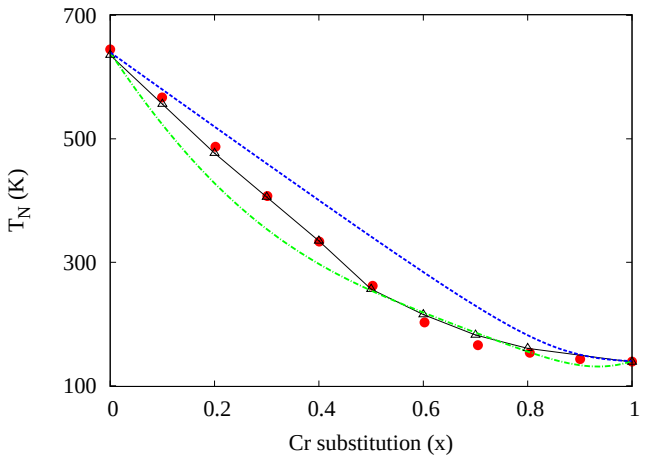

FIG. 4. (Color online) Néel temperatures as function of the fraction of Cr for[6] $YFe_{1-x}Cr_x0_3$ (red circles) and MC simulations (open triangles). The blue dashed line corresponds to Eq.(10) using the value of J_{12} reported by Dasari et al [6] and the green dot dashed line corresponds to Eq. (11) using the value of J_{12} reported by Kadomtseva et al [1]

B. $T = 0$ magnetization

In Fig.5 we show the modulus of the canted magnetization in the z direction (m_z) at $T = 0$ as function of the Cr content which is obtained from MC simulations in a ZFC process. We also plot the modulus of m_z obtained using Eq. (6) with the physical constants used in MC simulations. We see a good agreement between MC and the effective model at low and high chromium contents where the model is expected to work better. The local maximum at intermediate concentrations observed in MC simulations is related to a change in the sign of the magnetization. Like in the mean field model at intermediate concentrations the effect of the distributions of the DM bonds is important, and for this reason in this concentration range the effective model departs from MC simulations, in fact the effective model takes into account only averaged values in the distribution of the DM interactions. In addition, the effective canting due to the DM interactions can be approached using the following expression for the magnetization as function of the chromium content

$$m_z = \frac{1}{2}[m_{22}P_1[x]^2 + 2m_{12}J_{12}^2P_1[x]P_2[x] + m_{22}P_2[x]^2] \tag{12}$$

where m_{ij} is the averaged canted magnetization contribution of a pair of spins interacting through the DM interaction. Then, $m_{11} = 2\alpha_{11}m_1$, $m_{12} = \alpha_{12}(m_1 + m_2)$, and $m_{22} = 2\alpha_{22}m_2$. Here α_{ij} are the average canting angles between ions of type i and j (assuming low angles). According to Eq. (6), $\alpha_{ij} \simeq \frac{D_{ij}}{2J_{ij}}$ for $i = j$, and α_{12} is an effective parameter to be fitted. One can estimate as

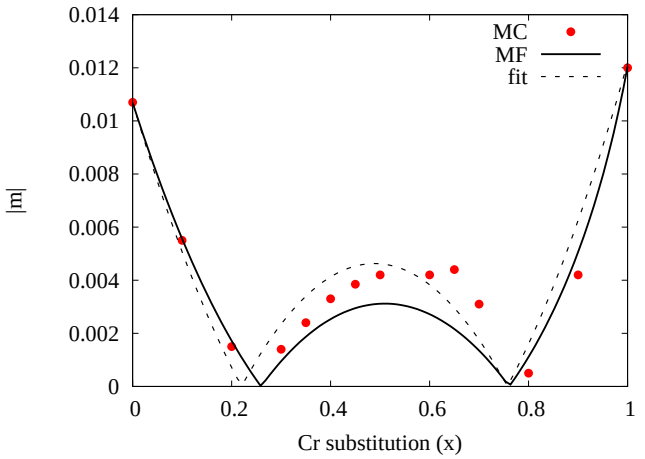

FIG. 5. (Color online) Module of the canted magnetization as function of the Cr content at $T = 0$ and zero applied magnetic field. Monte Carlo simulations (MC): red circles. Full lines correspond to the effective model Eq. (6) using the same parameters as in the simulation. The dashed lines correspond to a fit using Eq. (12).

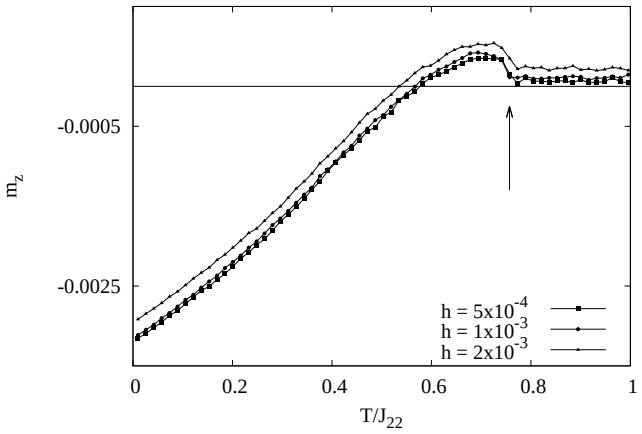

FIG. 6. Field cooling curves under different applied magnetic fields in the z direction for $x = 0.4$. The arrow indicates the ordering temperature obtained from the peak of the susceptibility. The applied field is in units of J_{22} i.e. $h = H/J_{22}$.

$\alpha_{12} = \frac{D_{12}}{2J_{21}}$ which turn in $\alpha_{12} = -0.0345$. The fixed parameters are $\alpha_{11} = 0.0203$ and $\alpha_{22} = 0.0107$. Fitting Eq. (12) to the MC data we obtain $\alpha_{12} = -0.0258$, showing the consistency of Eq.(12). Moreover, the negative magnetization can be understood from Eq.(12) as an effect of the negative sign of the DM interactions between Fe and Cr ions, which favors the canting of both ions in the negative z direction. Since Fe-Cr pairs are the majority at intermediate values of the Cr concentration x, the term in Eq.(12) associated with $m_{12} < 0$ is dominant and m_z becomes negative.

This local maximum has been reported in experiments carried out in single crystals of the $YFe_{1-x}Cr_xO_3$ compounds[1] where the low temperature magnetization is measured as function of the chromium content.

C. Magnetization reversal

In Fig. 6 we show the m_z component of the total magnetization as function of the temperature for $x = 0.4$ chromium content obtained by MC simulations using the parameters of the $LuFe_{1-x}Cr_xO_3$ compound already obtained in section II A. The cooling is performed under three different applied fields in the z direction; $h = H/J_{22} = 5 \times 10^{-4}$, 1×10^{-3}, and 2×10^{-3}. The arrow indicates the Néel temperature for this composition. We can observe reversal in the magnetization for this composition for the three applied fields. The magnetization increases with the applied field at low temperatures, although the compensation temperature appears to be almost independent of h, at least in the small range of values. In this case, $x = 0.4$, the compensation temperature is clearly smaller than the Néel temperature. We do not observe magnetization reversal for $x = 0.5$ and in fact in the composition range $x > 0.4$ the magnetization reversal is unstable. However, the shape of the curve obtained for $x = 0.4$ qualitatively reproduces the curves reported in the experiments for yttrium[5] ($YFe_{0.5}Cr_{0.5}O_3$) and lutetium[18] ($LuFe_{0.5}Cr_{0.5}O_3$) compounds. Moreover, the ratio between the compensation and Néel temperatures obtained in our simulation $T_{comp}/T_N = 0.76$ compares well with the experimental value[18] $T_{comp}/T_N = 0.83$.

In Fig. 7 we show FC magnetization curves with $h = 2 \times 10^{-3}$ for $x = 0.4$, and curves obtained through a mean field approach. Here we have measured in MC simulations separately the temperature dependence of the total magnetization of the Fe^{3+} ions and that of the Cr^{3+} ions. We can see that below the Néel temperature the magnetization due to the Fe^{3+} ions aligns in the direction of the magnetic field, while the magnetization due to the Cr^{3+} ions is opposite to the field. In this way, when the field breaks the inversion symmetry along the z axis the Zeeman energy is reduced due to the coupling of the larger magnetic moments of the Fe^{3+} ions. The different temperatures dependencies in the magnetization of Fe^{3+} and Cr^{3+} ions turns into the magnetization reversal. For lower compositions ($x \leq 0.3$) the Fe^{3+} ions are also aligned in the direction of the applied field but magnetization reversal is not observed because the contribution to the magnetization of Fe^{3+} is dominant.

In this figure we also show mean field curves which are obtained through Eq. (4) using a molecular field approximation for the dependence of the sublattice magnetization on the temperature. This approximation agrees very well with MC results for the sublattice magnetization. In the calculation of the mean field curves showed in Fig.

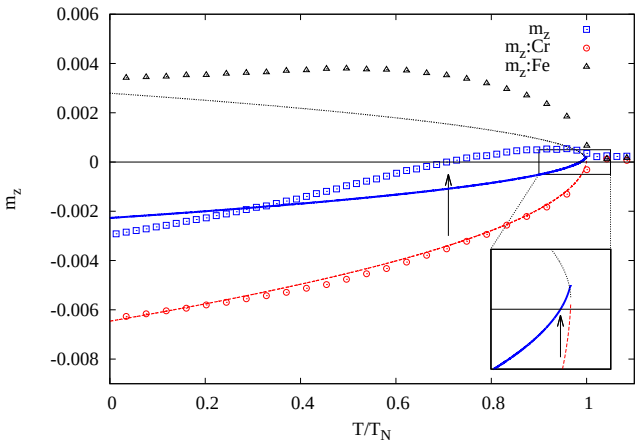

FIG. 7. (Color online) Field cooling curves with an applied fields in the z direction for $x = 0.4$. The applied field ($h = 0.002$) is the same for all the curves. The symbols with lines correspond to MC simulations and lines to MF results. MC simulations: chromium magnetization (black triangles), iron magnetization (red circles) and total magnetization (blue squares). MF calculations: chromium magnetization (black dotted line), iron magnetization (red dashed line) and total magnetization (blue continuous line). The arrows indicate the compensation temperatures in both cases, and the inset is a zoom of MF curves close to the ordering temperature.

Fig. 7 we used the same parameters than in MC results. These curves reproduce the features observed in MC results. However, in this case the compensation temperature (see inset) is much closer to the Néel temperature. From an analysis of the different energy term contributions, Eq. (4), we observed that close to the Néel temperature the Zeeman term is the most important hence the coupling with the field at high temperatures rules the magnetization process and induces the symmetry breaking. In the lower temperature range DM interactions prevail and convey the reversal of the magnetization.

III. DISCUSSION

Monte Carlo simulations using the proposed microscopic classical model reproduce the whole phenomenology of both $LuFe_{1-x}Cr_xO_3$ and $YFe_{1-x}Cr_xO_3$ compounds as the chromium content is varied. From these simulations it turns out that the superexchange interaction between Cr^{3+} and Fe^{3+} ions is lower than the superexchange interaction between Fe^{3+} and Fe^{3+}, and greater than the super-exchange between Cr^{3+} and Fe^{3+} ions i.e. $J_{22} > J_{12} > J_{11}$. From the fit of our experimental results with different mean field expressions, Eqs. (10) and (11) we obtained $J_{12} = 162$ K and $J_{12} = 11$ K, respectively.

These results show a big dispersion depending of the expression used to fit the experiments. In particular, the value obtained from MC simulations, $J_{12} = 106$ K, is in between this two values. The values of J_{12} available in the literature for Y perovskites $YFe_{1-x}Cr_xO_3$, also show an important dispersion. For instance, $J_{12} = 139$ K, when Eq. (10) is used in polycrystals[6] and $J_{12} = 38$ K has been reported in single crystals[1] using Eq. (11). Such large sensitivity to the details of the particular mean field approximation is not surprising in a solid solution, where the interplay between thermal fluctuations and the inherent disorder of the solution is expected to be very relevant to determine thermal properties. Consistently, the experimental results are better described by the MC simulations than by the MF expressions. Hence, we expect our estimation of J_{12} to be more reliable than the previous ones. In addition, our results suggest that the exchange constant (and therefore the general behavior) is not substantially affected by the substitution of yttrium by lutecium.

The zero temperature magnetization obtained from MC simulations in a ZFC process, which is due to the canting of the AFM spins in the z directions, is well approached by an effective coarse grain model in the range of low and high chromium contents as expected. A bump in the magnetization is observed in MC simulations at intermediate concentrations which is a signature of the magnetization reversal. This bump is also observed in the coarse grain approach but is less pronounced. The difference between MC simulations and the effective model at intermediate concentrations is expected since the coarse grain approach does not take into account information on the distribution of the ions in the lattice which is important at intermediate Cr concentrations.

Magnetization reversal is observed at intermediate chromium contents $x = 0.4$ in a ZFC process depending on the value of $D_{12}(\simeq 1.7\times10^{-2}J_{22})$. When the field is increased above a certain threshold MR disappear, and the magnetization points in the direction of the applied field in whole temperature range. The presence of magnetization reversal is very sensitive to the value of the DM interaction between Cr^{3+} and Fe^{3+} ions and also to the value of superexchange J_{12} interaction. We do not observe magnetization reversal in MC simulations at $x = 0.5$ such as is observed in experiments. This could be due to size effects which are particularly important in systems that includes disorder. In fact, the fields we used to obtain the ZFC curves (e.g. $h = 0.001$ correspond to $B \simeq 0.13$ T) are much greater that the ones used in experiments (e.g. $B \sim 0.01$ T). A reduction of the fields in MC is only possible in larger systems.

Summarizing, Monte Carlo simulations based in a Heisenberg microscopic classical model reproduce the critical temperatures observed in experiments. Besides this is a classical model, MC fit can provide a better estimation of J_{12} since in this model the random occupation of the Cr^{3+} and Fe^{3+} ions is taken into account. Regarding the phenomena of magnetization reversal, we found it for appropriated values of the superexchange and the Dzyaloshinskii-Moriya interactions at interme-

diate Cr concentrations. However, the mechanism for the appearance is subtle and further investigations are needed to shed light on this point.

ACKNOWLEDGMENTS

This work was partially supported by CONICET through grant PIP 2012-11220110100213 and PIP 2013-11220120100360, SeCyT–Universidad Nacional de Córdoba (Argentina), FONCyT and a CONICET-CNRS cooperation program. F. P. thanks CONICET for a fellowship. A. M. gratefully acknowledges a collaboration project between CNRS and CONICET (PCB I-2014). This work used Mendieta Cluster from CCAD-UNC, which is part of SNCAD-MinCyT, Argentina.

* billoni@famaf.unc.edu.ar
† fernandopomiro@gmail.com
‡ cannas@famaf.unc.edu.ar
§ christine.martin@ensicaen.fr
¶ antoine.maignan@ensicaen.fr
** rcarbonio@gmail.com

[1] A. M. Kadomtseva, A. S. Moskvin, I. G. Bostrem, B. M. Wanklyn, and N. A. Khafizova, Sov. Phys. JETP **45**, 1202 (1977).
[2] K. Yoshii and A. Nakamura, Journal of Solid State Chemistry **155**, 447 (2000).
[3] K. Yoshii, Journal of Solid State Chemistry **159**, 204 (2001).
[4] K. Yoshii, A. Nakamura, Y. Ishii, and Y. Morii, Journal of Solid State Chemistry **162**, 84 (2001).
[5] J. Mao, Y. Sui, X. Zhang, Y. Su, X. Wang, Z. Liu, Y. Wang, R. Zhu, Y. Wang, W. Liu, and J. Tang, Applied Physics Letters **98**, 192510 (2011).
[6] N. Dasari, P. Mandal, A. Sundaresan, and N. S. Vidhyadhiraja, EPL (Europhysics Letters) **99**, 17008 (2012).
[7] P. Mandal, C. Serrao, E. Suard, V. Caignaert, B. Raveau, A. Sundaresan, and C. Rao, Journal of Solid State Chemistry **197**, 408 (2013).
[8] Y. Ren, T. T. M. Palstra, D. I. Khomskii, E. Pellegrin, A. A. Nugroho, A. A. Menovsky, and G. A. Sawatzky, Nature **396**, 441 (1998).
[9] D. Treves, Phys. Rev. **125**, 1843 (1962).
[10] T. Moriya, Physical Review Letters **4**, 228 (1960).
[11] G. E. W. and S. J. A., Physical Review **90**, 487 (1953).
[12] M. N., D. K., and W. D. G., Physical Review Letters **4**, 119 (1960).
[13] P. R., J. Appl. Phys **29**, 253 (1958).
[14] Y. Ren, T. T. M. Palstra, D. I. Khomskii, A. A. Nugroho, A. A. Menovsky, and G. A. Sawatzky, Physical Review B **62**, 6577 (2000).
[15] J. Mao, Y. Sui, X. Zhang, Y. Su, X. Wang, Z. Liu, Y. Wang, R. Zhu, Y. Wang, W. Liu, and J. Tang, Applied Physics Letters **98**, 192510 (2011).
[16] P. Mandal, A. Sundaresan, C. N. R. Rao, A. Iyo, P. M. Shirage, Y. Tanaka, C. Simon, V. Pralong, O. I. Lebedev, V. Caignaert, and B. Raveau, Physical Review B **82**, 100416 (2010).
[17] a.K. Azad, a. Mellergård, S.-G. Eriksson, S. Ivanov, S. Yunus, F. Lindberg, G. Svensson, and R. Mathieu, Materials Research Bulletin **40**, 1633 (2005).
[18] F. Pomiro, R. D. Sánchez, G. Cuello, A. Maignan, C. Martin, and R. E. Carbonio, submitted (2016).
[19] A. K. Murtazaev, I. K. Kamilov, and Z. G. Ibaev, Low Temperature Physics **31**, 139 (2005).
[20] E. Restrepo-Parra, C. Bedoya-HincapiÃĺ, F. Jurado, J. Riano-Rojas, and J. Restrepo, Journal of Magnetism and Magnetic Materials **322**, 3514 (2010).
[21] E. Restrepo-Parra, C. Salazar-EnrÃŋquez, J. LondoÃśo-Navarro, J. Jurado, and J. Restrepo, Journal of Magnetism and Magnetic Materials **323**, 1477 (2011).
[22] T. Hashimoto, Journal of the Physical Society of Japan **18**, 1140 (1963).
[23] T. Moriya, *Magnetism III*, editing by g. t. rado and h. suhl ed. (Academic Press, New York, 1963).
[24] S. R. C., R. J. P., and W. H. J., J. Appl. Phys. **30**, 217 (1959).
[25] R. M. Hornreich, S. Shtrikman, B. M. Wanklyn, and I. Yaeger, Phys. Rev. B **13**, 4046 (1976).
[26] D. Treves, Journal of Applied Physics **36**, 1033 (1965).
[27] X. P. Yuan, Y. Tang, Y. Sun, and M. X. Xu, J. Appl. Phys. (2012).
[28] J. R. Sahu, C. R. Serrao, N. RAy, U. V. Waghmare, and C. N. Rao, J. Mater. Chem. (2007).